

# SOLID STATE SYNTHESIS AND X-RAY DIFFRACTION CHARACTERIZATION OF $\text{Pu}^{3+}_{(1-2x)}\text{Pu}^{4+}_x\text{Ca}^{2+}_x\text{PO}_4$

D. Bregiroux<sup>1,2</sup>, R. Belin<sup>1</sup>, F. Audubert<sup>1</sup> and D. Bernache-Assollant<sup>3</sup>

<sup>1</sup> Commissariat à l'Energie Atomique, DEN/DEC/SPUA, Cadarache, 13108 Saint Paul Lez Durance, France. E-mail : damien.bregiroux@cea.fr

<sup>2</sup> SPCTS, Université de Limoges, 123 avenue Albert Thomas, 87060 Limoges, France

<sup>3</sup> Ecole Nationale Supérieure des Mines, 158 cours Fauriel, 42023 Saint Etienne, France

## 1 INTRODUCTION

In the framework of the 1991 French law concerning nuclear waste management, several studies have been carried out in order to elaborate crystalline matrices for specific immobilization of the radionuclides. In the case of high level and long-lived minor actinides (Np, Am and Cm), which are high level and long-lived radioactive elements, monazite, a light rare earth (*Re*) orthophosphate with general formula  $\text{Re}^{3+}\text{PO}_4$  (with *Re* = La to Gd), has been proposed as a host matrix, thanks to its high resistance to self irradiation and its low solubility. Monazite crystallizes in the monoclinic space group  $\text{P2}_1/\text{n}$ . In this structure, trivalent cations ( $\text{Re}^{3+}$ ) could be substituted by an equivalent amount of bivalent ( $\text{A}^{2+}$ ) and tetravalent ( $\text{B}^{4+}$ ) cations, allowing the simultaneous incorporation of  $\text{Am}^{3+}$ ,  $\text{Cm}^{3+}$  and  $\text{Np}^{4+}$ . According to Podor's work<sup>1</sup>, the limit of a tetravalent element incorporation in monazite is related to its size in the ninefold coordination ( $\text{R}^{\text{IX}}$ ).  $\text{Re}^{3+}_{1-2x}\text{A}^{2+}_x\text{B}^{4+}_x\text{PO}_4$  exists in the monazite structure if  $1,216\text{\AA} \geq \text{R}_{\text{average}} \geq 1,107\text{\AA}$  and  $1,238 \geq \text{R}_{\text{ratio}} \geq 1$  with

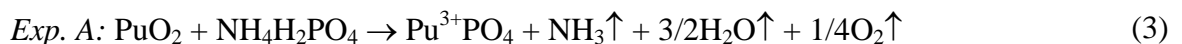
$$\text{R}_{\text{average}} = (1-2x)\text{R}_{\text{Re}^{3+}}^{\text{IX}} + x\text{R}_{\text{A}^{2+}}^{\text{IX}} + x\text{R}_{\text{B}^{4+}}^{\text{IX}} \quad (1)$$

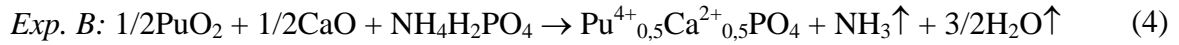
$$\text{R}_{\text{ratio}} = \frac{(1-2x)\text{R}_{\text{Re}^{3+}}^{\text{IX}} + x\text{R}_{\text{A}^{2+}}^{\text{IX}}}{(1-2x)\text{R}_{\text{Re}^{3+}}^{\text{IX}} + x\text{R}_{\text{B}^{4+}}^{\text{IX}}} \quad (2)$$

The present work deals with the incorporation of the  $\text{Pu}^{4+}/\text{Ca}^{2+}$  couple in the monazite structure by solid state synthesis. According to the equation (1) and (2), the maximum incorporation is  $x=0.43$ , with  $\text{Re}^{3+}=\text{Pu}^{3+}$ , leading to a compound with the formula  $\text{Pu}^{3+}_{0.14}\text{Pu}^{4+}_{0.43}\text{Ca}^{2+}_{0.43}\text{PO}_4$ .

## 2 MATERIALS AND METHODS

The monazite powders were prepared according to the following reactions:





Both compounds were prepared on a few milligrams scale. Starting materials were homogenized by manual grinding in an agate mortar and then fired in a platinum crucible at 1400°C for 2h under air atmosphere in an alumina tubular furnace. The whole process was repeated in order to obtain homogeneous materials. Powders were characterized by X-ray diffraction at room temperature using a high-resolution Siemens D5000 X-ray diffractometer with a curved quartz monochromator and copper radiation from a conventional tube source.

### 3 RESULTS AND DISCUSSION

#### 3.1 Structure analysis

X-ray diffraction patterns of the two resulting materials are shown on Figure 1. For both, it was found that the plutonium phosphate crystallizes in the monazite structure as expected. For the experiment A, a secondary phase was identified as a tetravalent plutonium phosphate  $\text{Pu}^{4+}\text{P}_2\text{O}_7$ . This suggests that under air atmosphere, the  $\text{Pu}^{4+}$  is not completely reduced into  $\text{Pu}^{3+}$ . This result is in agreement with those of Bamberger<sup>2</sup> who showed that the apparent stability of  $\text{PuP}_2\text{O}_7$  in air is due to its very slow rate of decomposition into  $\text{PuPO}_4$ . On the other hand, the result of the experiment B is single phased.

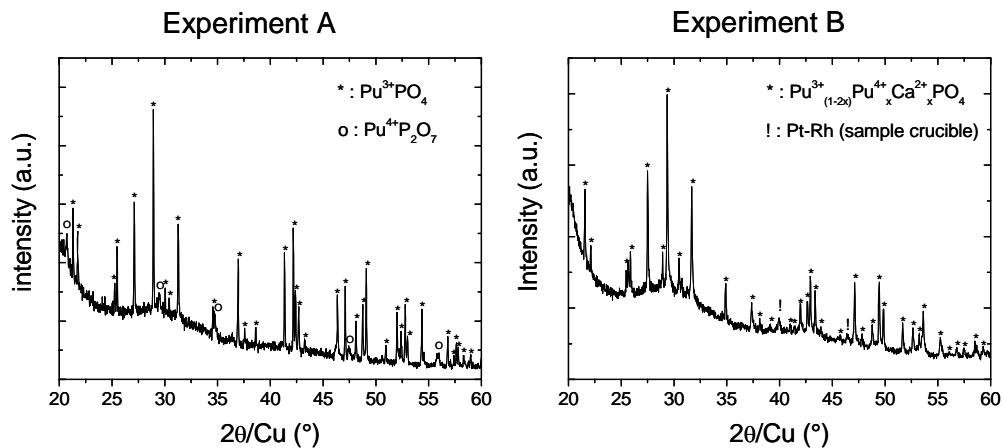


**Figure 1** X-ray diffraction diagrams of the synthesized powders

Lattice parameters of the monazite structure are given in table 1. They are lower for monazite B than for monazite A. Since  $\text{Pu}^{4+}$  and  $\text{Ca}^{2+}$  are smaller than  $\text{Pu}^{3+}$ , one can assume that  $\text{Pu}^{4+}$  was incorporated in the monazite structure.

**Table 1** Cell parameters of the synthesized monazite

	a (nm)	b (nm)	c (nm)	$\beta$ (°)
<b>Monazite A</b>	0,675	0,697	0,643	103,64
<b>Monazite B</b>	0,667	0,687	0,636	103,99

#### 3.2 Determination of the chemical composition

Recently, Terra showed that for  $\text{La}^{3+}_{1-2x}\text{Th}^{4+}_x\text{Ca}^{2+}_x\text{PO}_4$  and  $\text{Ca}^{2+}_{0.5}\text{Th}^{4+}_{0.5-y}\text{U}^{4+}_y\text{PO}_4$  solid-solutions, the variation of the cell parameters versus x and y is linear from 0 to 0.5<sup>3</sup>. If we assume a similar evolution with the  $\text{Ca}^{2+}_{0.5}\text{Np}^{4+}_{0.5-y}\text{Pu}^{4+}_y\text{PO}_4$  solid solution, the cell

parameters of  $\text{Ca}^{2+}_{0.5}\text{Pu}^{4+}_{0.5}\text{PO}_4$  (round points on Figure 2) can be extrapolated from the parameters of the two compositions of the  $\text{Ca}^{2+}_{0.5}\text{Np}^{4+}_{0.5-y}\text{Pu}^{4+}_y\text{PO}_4$  solid-solution reported by Tabuteau<sup>4</sup> (Table 2). The  $\text{Pu}^{4+}$  incorporation rate in the monazite structure can thus be deduced from the cell parameters (square points on Figure 2) of the monazite B powder. Results show that the monazite B chemical composition ( $\text{Pu}^{3+}_{0.4}\text{Pu}^{4+}_{0.3}\text{Ca}^{2+}_{0.3}\text{PO}_4$ ) is less than expected. According to our recent work on the incorporation of  $\text{Ce}^{4+}$  in the monazite structure<sup>5</sup>, residual  $\text{Ca}^{2+}$  should be incorporated in a secondary phase  $\text{Ca}_2\text{P}_2\text{O}_7$ . This compound was not observed by X-ray diffraction most likely because of the unfavourable signal to noise ratio.

**Table 2** Lattice parameters of  $\text{Ca}^{2+}_{0.5}\text{Np}^{4+}_{0.5-y}\text{Pu}^{4+}_y\text{PO}_4$  solid solution

	a (nm)	b (nm)	c (nm)	$\beta$ (°)
$\text{Ca}_{0.5}\text{Np}_{0.5}\text{PO}_4$	0.6666	0.6854	0.6370	104.11
$\text{Ca}_{0.5}\text{Np}_{0.35}\text{Pu}_{0.15}\text{PO}_4$	0.6649	0.6840	0.6351	104.14

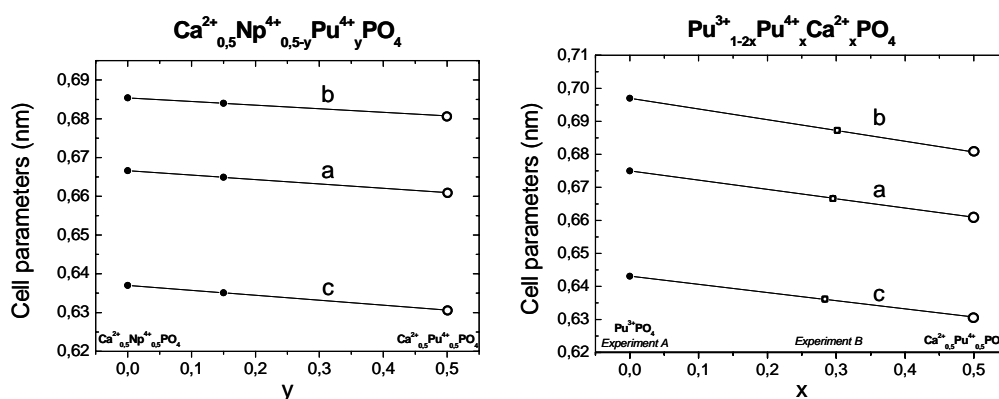


**Figure 2** Lattice parameters of  $\text{Ca}^{2+}_{0.5}\text{Np}^{4+}_{1-y}\text{Pu}^{4+}_y\text{PO}_4$  and  $\text{Pu}^{3+}_{1-2x}\text{Pu}^{4+}_x\text{Ca}^{2+}_x\text{PO}_4$  solid solution versus y and x

#### 4 CONCLUSION

The solid state synthesis of  $\text{Pu}^{3+}_{(1-2x)}\text{Pu}^{4+}_x\text{Ca}^{2+}_x\text{PO}_4$  under air was carried out.  $\text{Pu}^{3+}\text{PO}_4$  was not obtained as a single phase and the maximum incorporation of  $\text{Pu}^{4+}$  in the monazite structure was found to be around  $x = 0.3$ . To complete the present work, the same experiments will be carried out under inert atmosphere.

#### References

- 1 R. Podor and al. *Experimental study of Th-bearing  $\text{LaPO}_4$  (780°C, 200MPa): Implications for monazite and actinide orthophosphate stability*, Amer. Miner. **82**, pp. 765-771 (1997).
- 2 C.E. Bamberger and al. *Synthesis and characterization of crystalline phosphates of plutonium(III) and plutonium(IV)*, J. Less-Common Met. **97**, pp. 349-356 (1984).
- 3 O. Terra. *Incorporation d'actinides tétravalents dans trois matrices phosphatées: britholite, monazite/brabantite et Phosphate-Diphosphate de Thorium*, thèse de l'Université d'Orsay, Paris XI (2005).
- 4 A. Tabuteau and al. *Monazite-like phases containing transuranium elements (neptunium and plutonium)*, J. Mater. Sci. Lett. **7**, pp. 1315-1317 (1988).
- 5 D. Bregiroux and al. *Study of tetravalent cerium incorporation in the monazite structure*, Atalante 2004 Conference, Nîmes, France (2004)